

# Microfluidic device for single-cell analysis and gradient generation

Marta Amaral<sup>1</sup>

<sup>1</sup> Instituto Superior Técnico, Av. Rovisco Pais, 1049-001, Lisbon, Portugal

---

**Abstract:** Cellular behavior has been investigated by utilizing *macroscale* methods that measure average values over a population of cells.

The present study focused on the development of a microfluidic device for single-cell analysis and gradient-generation.

A hybrid PDMS/glass microfluidic device was fabricated using the Soft Lithography process. The master mold was fabricated using a new technique of Rapid Prototyping in which the master mold is directly fabricated by double exposure on a Direct Laser machine (DWL) without the need of any photomask. Approaches to localize the same cell over long periods were improved as well as a new methodology that force cells to enter the microchannels.

The conceived microfluidic platform was applied to study *Saccharomyces cerevisiae* yeast cells carrying out two fluorescent proteins, one of them fused with  $\alpha$ Syn, a protein related to Parkinson's Disease.

The results obtained demonstrate the effectiveness of the device to establish a suitable environment for cell growth and protein expression as well as the capacity to visualize individual cells.

This work also demonstrates an approach to generate chemical gradients by using microchannels featured alongside two main reservoirs. The creation of a stable gradient inside the channels using the fluorophore FITC was achieved for 2-3 hours despite being different from the theoretically expected.

**Keywords:** Microfluidic device, PDMS, Microchannels, Soft lithography, Alpha-Synuclein Chemical Gradients

## 1. Introduction

Microfluidics is the science and technology of systems that process or manipulate small amounts of fluids, using channels with dimensions of tens to hundreds of micrometres [1].

Microfluidics systems have the potential for wide applications, including advances in point-of-care diagnostics, bioterrorism detection, drug discovery, biotechnology, pharmaceuticals and life sciences [2].

The great development of this new distinct field lies in the fact that microfluidic devices require small amounts of sample and reagent for each process leading to greater efficiency of use of chemical or biochemical reagents. Other advantages include low production costs per device thereby allowing for disposability; high throughput synthesis and screening of biological species and drug targets; parallel processing of samples; fast sampling times; portability for in situ use; accurate and precise control of samples; low power consumption; and versatile format for integration of various detection schemes thereby leading to greater sensitivity [3].

Microfluidic devices were first developed in the 1990s and were initially fabricated in silicon and glass using the traditional techniques borrowed from the semiconductor industry, specifically photolithography and etching techniques, because these technologies were available and highly developed, although they are also expensive and inflexible [4].

Newly alternatives appeared in order to overcome the drawbacks of such materials. Among those alternatives have emerged ceramics, plastics, and polymer-based materials. Much of the exploratory research in microfluidic systems has been carried out in poly(dimethylsiloxane), PDMS.

The main approach to the fabrication of microfluidic devices is based on the techniques of Soft Lithography, specially Rapid Prototyping and Replica Molding [4,5,6,7]. Briefly this technique starts with the mask preparation and mold fabrication (Rapid Prototyping). Rapid prototyping begins with the creation of a design for the future device using a CAD program. This design will then be patterned by photolithography on a substrate to serve as the photomask. Afterwards, such photomask by contact photolithography will then produce a positive relief of photoresist on silicon wafer (master). Once the master is fabricated, the patterned is formed in PDMS by replicate molding. Using this technique, PDMS is poured onto the master, hardened using heat or ultraviolet light, and peeled off to yield a negative replica of the master mold.

Many recent studies has been a focus on the development and utilization of single-cell experimental techniques [8,9,10]. Cellular heterogeneity has been observed in a wide variety of cell types ranging from simple bacterial cells to more complex mammalian cells. Any population

of cells will exhibit some degree of variability, and genetic differences are one of the main factors responsible for cellular heterogeneity.

Traditional microscopy experiments can track gene expression dynamics in individual cells, but can only monitor a relatively small population of cells. On the other hand, microfluidics can be used to track gene expression changes in individual cells, enable large populations of cells to be monitored, and allow the precise control of the cellular microenvironment.

Other important approach that has been studied using microfluidic platforms is the development of stable biomolecular gradients.

Such gradients have been used in many different fields, for example to examine the effects of various biomolecule gradients on the chemotaxis of neutrophils [11], bacteria [12,13] sperm [14], breast cancer cells [15], or to infect cells with graded concentrations of virus [16].

In the present work the microfluidic device was used to analyse single *Saccharomyces cerevisiae* cells. *Saccharomyces cerevisiae* is the most thoroughly investigated eukaryotic microorganism and it has been the model system for much of molecular genetic research because the basic cellular mechanics of replication, recombination, cell division and metabolism are generally conserved between yeast and larger eukaryotes, including mammals [17].

One of the most important reasons for the applicability of *S. cerevisiae* within the field of biotechnology is its susceptibility to genetic modifications by recombinant DNA technology, which has been even further facilitated by the availability of the complete genome sequence of *S. cerevisiae*, published in 1996 [18].

In this project a particular protein was studied, Alpha-Synuclein, in order to test the effectiveness of the microfluidic device to visualize and quantify the expression levels of proteins when subject to the action of a soluble component.  $\alpha$ -synuclein is a protein implicated in the regulation of dopamine release and transport.

Recent studies indicate that negative influences can turn the protein alpha-synuclein into a major contributor of the movement-impairing disorder, Parkinson's disease [19,20].

Outeiro and colleagues [21] had used *Saccharomyces cerevisiae* to establish basic aspects of both normal and abnormal  $\alpha$ Syn biology due to the strong conservation of protein folding and membrane trafficking between yeast and higher eukaryotes.

This paper presents a new microfabrication technique to fabricate microchannels with widths coincident to that of cells of interest (5-10 $\mu$ m), and thus enabling the analyses of single-cells. A new methodology to force cells to enter the microchannels was also developed. The

microfluidic platform was applied to analyse single *S. cerevisiae* cells in terms of cell growth and protein expression levels. *S. cerevisiae* cells were carrying  $\alpha$ Syn, a protein related to Parkinson's disease.

The microfluidic platform was adapted to generate stable gradients for 2.5 hours across microchannels featured alongside two main reservoirs

## 2. Materials and methods

### 2.1. Fabrication of the microfluidic device

The microfluidic platform was fabricated using the Soft Lithography technique.

The mask design was created using the AutoCAD 2005 program. The design included 5 groups of channels with a length of 1cm. Each group of channels had widths between one hundred and five microns (100, 50, 20, 10 and 5 $\mu$ m). Along all the channels a ruler was added to the mask design so that it could be easier to localize a particular cell along the time.

A new microfabrication technology was implemented to fabricate the master mold, using the positive photoresist PFR 7790G 27cP (from JSR), and the steps are given by the following figure:

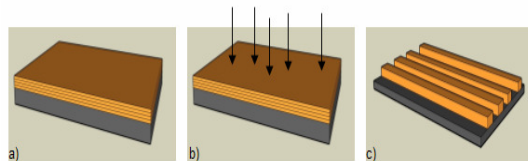


**Figure 1** - Master mold fabrication using the positive photoresist PFR 7790G 27cP. a) Coating of 4 layers of positive PR. b) DWL double exposure. c) Master mold after development.

Before resist coating, the silicon substrate was vapor primed with HMDS for 30 minutes to improve the adhesion of the resist to the substrate. Afterwards, the spin coating step (2800 rpm for 40s to have a thickness of 1.5 $\mu$ m) and the bake step (85 $^{\circ}$ C) were repeated four times in order to achieve a thickness layer of 6 $\mu$ m. After each bake step, the Si sample needed to cool for 10 minutes until room temperature was reached again. The sample was exposed in DWL (Direct Write Laser) using a 422nm wavelength laser (near ultra-violet light) but due to the higher thickness of the photoresist layers, it was necessary to increase the power of the machine to 100%. Furthermore, the sample was subjected to two consecutive exposures to ensure that all the layers were affected by the laser beam. The development step was made in short steps of 20 seconds, and the pattern was checked in the microscope to verify if the sample was perfectly developed.

Two pieces of silicon (20mm x 5mm x

0,7mm) were bonded to the master mold to serve as reservoirs, according to the alignment marks in the mold, using double face tape (Figure 2). The microchannels, after the Si pieces having been bonded, have a final length of 0,5 cm.

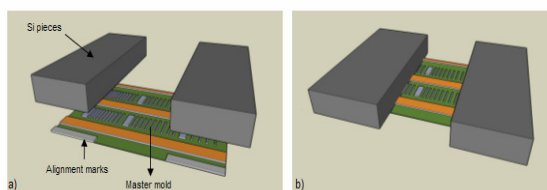


**Figure 2** – Master mold with two pieces of silicon acting as the mold for the reservoirs.

To improve the efficiency of the mold fabrication three dies in the same mold were done to allow the fabrication of three PDMS replicas at the same time, thus decreasing the time spent on the microfluidic device fabrication.

The PDMS formulation used, Sylgard™ 184 (Dow Corning; Midland, MI), is composed by a liquid silicon rubber base and a curing agent. The base and curing agent were measured in a 10:1 ratio by weight, according to the Sylgard 184 silicone elastomer datasheet [22], and mixed thoroughly by hand for about 2 minutes. Mixture was then degassed in a desiccator under vacuum for 1 hour. The mold was put over a flat surface (plastic container) and PDMS was poured over the mold and cured in an oven for 1 hour at 60 °C. After curing the elastomer, the device was released by peeling from the mold and cut with the right dimensions in order to be assembled and bonded to a glass microscope slide.

Before mounting the PDMS replica on a glass microscope slide they were both cleaned with HCl 32% from Merck (1:5) for 8 minutes and then rinsed with IPA. The next step involved the irreversibly bonding between these two surfaces using the Corona Discharge (model BD-20AC from Electro-Technic Products Inc), which will oxidize PDMS and thus allow a permanent bond between the PDMS replica and substrate to be formed.

After the PDMS/glass microfluidic device was made with close reservoirs, it was necessary to open vias in order to connect the microfluidic device with the tubes that constitute the external fluidic system. First, two openings were punched using a 20 gauge blunt needle to insert metal connectors in the PDMS. Before connecting the PDMS to the outside fluidic system it was important to do a Corona Discharge to transform the hydrophobic surface of the channels/reservoirs into a hydrophilic one. This treatment was made introducing a small electrode (a needle type electrode) inside the reservoirs and the power supply was turned on for 10 seconds. Immediately after Corona Discharge both wells

were completely filled with water using a 1 ml syringe to prevent the hydrophobicity recovery. One metal connector was then inserted in one of the reservoirs and connected to the outside by a 20 ga polyethylene catheter tube. A vacuum was made in that reservoir, using a 1 ml syringe and pulling on the plunger carefully, to force the liquid to enter through the channels. The other connector was then inserted in the opposite reservoir (jointly with the polyethylene tube) and both connectors were glued with silicon gel to avoid any fluidic escape. They were placed sideways to the device to facilitate the visualization on the microscope (Figure 3).

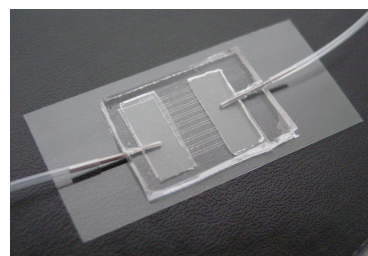


**Figure 3** – Microfluidic device with tubage responsible for the outside fluidic system.

## 2.2. Yeast cells

The yeast cells used in this project were provided by the group of Dr. Tiago Outeiro at the IMM (Instituto de Medicina Molecular).

Transformations of yeast were carried out using the standard lithium acetate procedure. This process was performed to introduce in *Saccharomyces cerevisiae* strain W303.1A (*MATa*; *can1-100*; *his3-11 15*; *leu2-3 112*; *trp1-1*; *ura3-1*; *ade2-1*) [23] two 2 $\mu$  plasmids, one with GFP- $\alpha$ Syn fusion protein under the control of a galactose-inducible promoter and the other with a RFP protein under the control of a methionine-repressible promoter.

Another strain was also used, VSY72 (a kind gift from Vicente Sancanon, Gladstone Institute of Neurological Disease, San Francisco, USA) made in the W303.1A background and has the following genotype: *MATa*; *can1-100*; *his3-11 15*; *leu2-3 112*; *ade2-1*; *GAL1pr-SNCA(WT)-GFP::URA3*; *GAL1pr-SNCA(WT)-GFP::TRP1*. On this strain two copies of the SNCA (WT) were inserted directly in the genome, and these genes encode  $\alpha$ Syn-GFP fusion protein.

Before starting with the experiments, yeast strains were pre-grown for 24 hours at 30 °C in raffinose medium. The cells used in the experiments were in the exponential phase and concentrated to a final OD<sub>600</sub> of approximately 3.4 by short centrifugation. Before loading the cells into the device a vigorous vortex was made.

Before introducing the cells in the reservoirs they were previously emptied due to the fact that

they were full of water to avoid hydrophobic recovery. The solution with the cells was then introduced through the inlet reservoir and a vacuum was applied through the outlet (connecting one 1ml syringe with the polyethylene tube and pulling on the plunger carefully) to force them to flow along the channels.

### 2.2.1. Cell growth within microchannels

To compare the growth rate of yeast cells within microchannels and in traditional *macro* cultures, the cells were introduced in the microfluidic device, and some cells in different channels were selected and their positions registered (with the help of the *ruler*).

Two different experiments were performed with the two different yeast strains available. In the first experiment, we used *Saccharomyces cerevisiae* strain W303.1A. Images were acquired every 1.5 hours for 4.5 hours. After acquiring such images, the device was placed over a heated aluminium plate at 30°C until the time new images were acquired. In the other experiment, cells carrying two copies of the  $\alpha$ Syn-GFP fusion protein inserted in the genome were used (VSY72). Cells were grown overnight in an incubator, at 30°C, and were only visualized after 18 hours.

### 2.2.2. $\alpha$ -Syn expression induction with Galactose

The two yeast strains available, W303.1A and VSY72, were used to visualize the expression levels of  $\alpha$ Syn-GFP fusion protein (GFP- $\alpha$ Syn in the case of the strain W303.1A) when stimulated with galactose inducer.

Cells were previously centrifuged and resuspended in galactose (1%) medium. Immediately after, the cells were inserted in the microfluidic device using one 1ml syringe. The device was positioned on the stage of the microscope, and some cells in different channels were selected to study the protein expression levels along time. The location of the cells over long periods was achieved by the *ruler* near the channels which allows the rapid recognition of such cells. Cells were then imaged with a Axiovert 200 model inverted microscope from Zeiss equipped with a digital camera AxioCam MRm from Zeiss every 1.5 hours. The microscope was equipped with GFP and RFP filters. The microscope images were 63x magnifications.

### 2.3. Generation of a Stable Gradient inside the channels

The basic design of the microfluidic device developed in this project consists of two

reservoirs connected by a number of microchannels. The dimensions of the channels were significantly smaller (6  $\mu$ m high and 5-10  $\mu$ m wide) than the reservoirs (700  $\mu$ m high and 20 mm wide). Due to this size difference, we expected that the fluidic resistance of the microchannels would be much higher than that of the reservoirs, thus minimizing the likelihood of convection through the microchannels. Diffusion would thus be the predominant mode of transport across the microchannels. When a molecular species is introduced in one of the reservoirs and buffer in the other, molecules diffuse across the microchannels and generate a gradient.

The Experimental Setup consists of 1 syringe pump carrying two syringes, each one connected to the reservoirs of the microfluidic device by polyethylene tubes. In the other side of the reservoirs they are connected to *ependorf* tubes, in which the molecular species (dye) and the buffer are stored (Figure 4).

Gradients were characterized using fluorescence microscopy. Carbonate buffer was loaded into one *ependorf* tube for the reservoir and a 389mM FITC solution (from Sigma-Aldrich) in NaHCO<sub>3</sub> was loaded into the other *ependorf* tube for the opposite reservoir. Flow rates of 5.5  $\mu$ L/min were maintained by withdrawing the fluids from the reservoirs using the syringe pump. Gradient evolution was monitored. Images were analyzed using ImageJ program. For each image, the fluorescence intensity was measured and the background was subtracted.

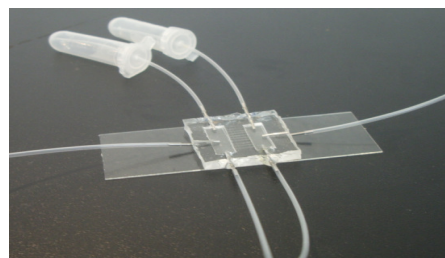


**Figure 4** – Microfluidic device adapted for the creation of stable gradients inside the microchannels.

## 3. Results and Discussion

### 3.1. Microfluidic Device

The method used to fabricate the master mold involved the use of the photoresist PFR 7790G 27cP. This photoresist is usually used in DWL machine for mask making and direct writing. However, the state of the art technology of this system can also create complex 3D structures in thick photoresist. Each layer of this photoresist could have the maximum thickness (according to the spin speed) of 1.5 $\mu$ m. Thereby, to achieve an appropriate thickness so that the cells could enter

the channels, an overlapping of 4 layers of this photoresist was necessary.

The implementation of this method to make the mold had the great advantage of creating the required pattern given by the input file, without the need of any mask. With this method the microchannels with widths between one hundred and five micrometers were obtained with a very high precision, as it is shown in Figure 5.

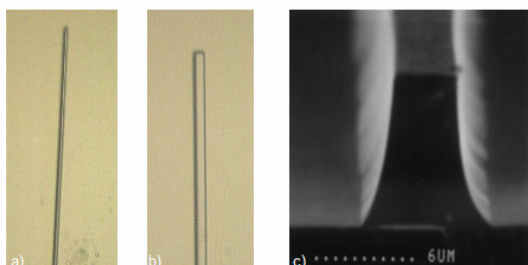


Figure 5 - Microchannels made of 4 layers of photoresist PFR 7790G 27cP. a) Microchannel with a width of 5 $\mu$ m and b) 10 $\mu$ m. c) SEM photograph showing the profile of a microchannel.

Some preliminary cell-experiments were performed to verify which channel size would be the optimal one to visualize single *Saccharomyces cerevisiae* cells (data not shown). The cells in the bigger channels (100, 50 and 20 $\mu$ m) did not adhere on the glass substrate or on the PDMS sidewalls but simply went along the channels without stopping. In the channels with widths down to 20 $\mu$ m the cells entered the channels but these channels offered more resistance when they passed, which prevented these cells from leaving the channels. Furthermore, the PDMS sidewalls usually present some irregularities that reduce the brownian motion of the cells. Therefore, it was possible to conclude that to analyse single yeast cells microchannels should have widths between 10 and 5 $\mu$ m.

As described in 2.1, rectangular pieces of silicon were used to act the mold for the inlet and outlet reservoirs. Ideally, the device should have been done all integrated by soft lithography including the reservoirs. However, using the methodology of mold fabrication described in 2.1 it was not possible to achieve a photoresist thickness greater than 6 microns and thus, to obtain reservoirs with a significant capacity, the area of these ones had to be very high. Using reservoirs with great areas when compared to the height, PDMS sag and close off the fluidic channels when in contact with the glass substrate. It was described in the literature [10] that to avoid the collapse of the reservoirs, one could add some support structures (pillars) uniformly distributed along the reservoirs. However, the capacity of the reservoirs would decrease significantly and for the aim of this project this situation would be disadvantageous.

Another possibility could be the use of photoresists (mainly SU-8) with different standard viscosities to have multi-height structures in the master mold according to the applications desired [24,27]. However, this method was much more complex and the photoresist used to fabricate the mold in this project was only available in INESC MN in one standard viscosity.

Using the methodology developed in the present project to do the mold for the reservoirs, they have much higher capacity when compared to reservoirs made of any photoresist due to the higher thickness. This capacity could also be increased/decreased by simply changing the dimensions of the silicon pieces used to make the reservoirs.

Usually, in microfluidic devices the reservoir holes were simply punched through the PDMS using sharpened needles, thereby such reservoirs would be open to the atmosphere [24,25,26]. Using the methodology developed in this project to make the mold for the reservoirs, the device has close reservoirs avoiding any cell contamination. Furthermore, a fully closed microfluidic device is also very important in cells experiments because it allows a completely controlled environment. The major advantage of this microfluidic device, together with the tubes that constitute the external fluidic system, is the capability of making a vacuum inside it, which force the fluid/cells to enter the microchannels.

Despite the fact that this method was very efficient for the goals of this project, it could have some disadvantages that incapacitate its use for more specific and complex patterns. For example, channels with small lengths ( $\leq 1000\mu$ m) could be difficult to obtain due to the proximity of the silicon reservoirs therefore one has to be very careful when peeling the PDMS over the mold. Using a microfluidic design similar to the one performed in this project it is very difficult to guarantee that all the channels were hydrophilic after Corona Discharge because this treatment was made on the reservoirs and not channel by channel and thus it was impossible to ensure that such treatment covered all the channels.

### 3.2. Cell Experiments

To find the optimal optical density in which the cells entered the microchannels and stayed as sparse as possible, firstly, an  $OD_{600}$  around 10 tested. After applied vacuum to force the cells to go through the channels in many of them cells came into the channels in big clusters which made their movement along such channels difficult. For this reason, in all the further experiments an  $OD_{600}$  of approximately 3.4 was used and before introducing the cells into the device a vigorous

vortex was applied to separate them from each other (Figure 6).

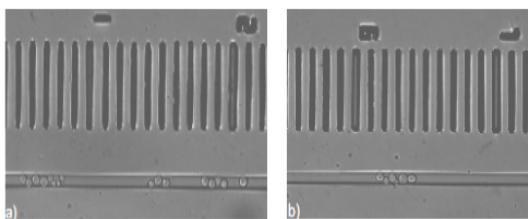


**Figure 6** - Yeast cells inside microchannels with an  $OD_{600}$  of 3.4 and after a vigorous vortex.

For experiments involving the visualization of individual cells over time, the *ruler* made close to each channel proved to be a very efficient way to localize such cells. During these experiments, some channels were selected according to the best cell distribution (and their locations registered), and images of the cells inside these channels were acquired over long times.

Some cells were weakly adherent to the glass substrate and therefore during the time of the experiments some of them changed their positions and it was difficult to localize them again. Researchers have been very inventive in developing mechanical obstacles or barriers to sieve a particular object from a fluid suspension by providing a passage for the fluidic only [10]. This hydrodynamic trapping has the advantages that cell immobilization is rapid compared with chemical trapping and that the devices are often simple and inexpensive.

Although the microfluidic channels made in this project work as traps due to their small widths, a simple approach was performed to test the efficiency of a simple trap. A new mold was fabricated in which some channels presented small traps in order to narrow them in particular places like it was shown in Figure 7.

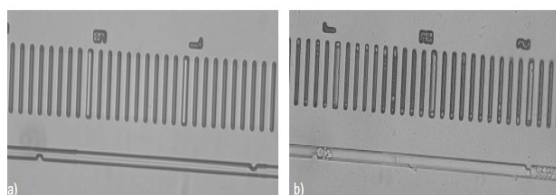


**Figure 7** - Hydrodynamic traps. a) Microchannel with 2 traps. b) Yeast cells trapped inside a microchannel.

This simple method had shown to be efficient to trap cells, however one has to be more careful when working with these microchannels because if a cluster of cells get stuck in the first trap, no more cells could enter the channels and they start to accumulate at the beginning of this channel.

### 3.2.1. Cell growth within microchannels

The division time of wild type cells is about 120 minutes (in minimum medium) in traditional

culture flasks (S.Tenreiro, personal communication).

In the first cell growth experiment (using the strain W303.1A) it was found that, after three hours of experiment, yeast cells divided once, twice or even did not divide at all. These results were somewhat according to the expectations because all the cells were in different stages of growth and thus it was not expected that they divided all at the same time that is to say in a synchronized way. Besides that, individual cells present different cellular rhythms that could also explain such variability on division time.

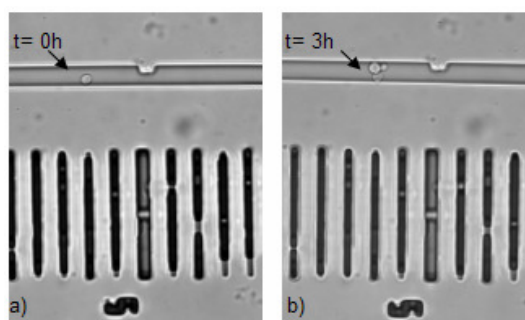


**Figure 8** - Yeast W303.1A cells growth within microchannels. a) Individual cells were selected and b) the same cells were visualized after 3 hours

Compared to traditional cell cultures, in microfluidic platforms we were able to visualize relatively small number of cells, however, because a group of cells can more easily maintain a local environment within microchannels than in *macroscale* culture flasks, cells can grow significantly slower in microchannels [27,28].

The same experiment was performed to visualize cells growth within the microchannels but this time the cells used were the ones with two copies of the genes that encode  $\alpha$ -syn-GFP fusion protein inserted in the genome (strain VSY72), to compare the division times between this strain and wild type cells. Cells were grown in galactose medium to express  $\alpha$ -syn-GFP protein to see if they express this protein at the same intensity in cells genetically identical.

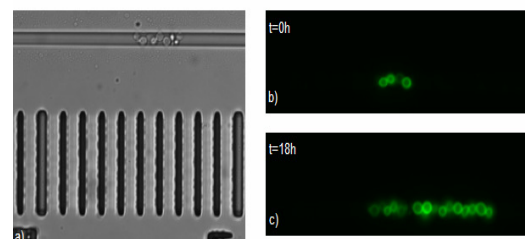


**Figure 9** - Yeast VSY72 cell growth within microchannels expressing  $\alpha$ Syn-GFP fusion protein. a) Visible micrograph of cells previously selected within microchannels at t=0h. b) Fluorescence micrographs of the same cells at t=0h and c) t=18h.

Before examining the division time of the cells it is important to observe that  $\alpha$ Syn-GFP is clearly located in the plasma membrane in all the cells (Figure 8), after 18 hours of incubation which led us to conclude that the cells were viable inside microchannels and were constantly induced by galactose medium. This and other assays helped us to prove the effectiveness of the microchannels as an appropriate environment for the study of single cells.

The results provided a division time of 4,5 hours. We verified that when overexpressed (two copies),  $\alpha$ Syn inhibited growth if we compare to the division time of wild type cells. The inhibition of growth when overexpressed may be evidence of the toxicity of  $\alpha$ Syn as observed before by Outeiro and colleagues [21].

This type of studies, when we pretend to observe the successive generations of the same cell, is an added value of this type of microfluidic devices since we were able to visualize many individual cells along different channels for long periods in the same experiment. In *macrocultures*, this kind of studies was only possible to perform if we have a couple of cells in the same field since it is not possible to change it because it would be very difficult to localize the same cells again.

When a certain device is being developed for biological studies, it is very important to recall that all biological species have an optimal temperature range in which they grow best. Particularly, *S. cerevisiae* works best at about 30°C. Therefore, the microfluidic setup should have incorporated a system to control temperature with high precision within microchannel environments.

### 3.2.2. $\alpha$ -Syn expression induction with Galactose

The expression of  $\alpha$ Syn protein was induced in galactose both in the strains W303.1A and VSY72.

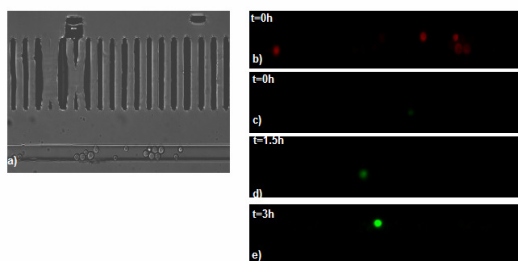


**Figure 10** - Expression levels of GFP- $\alpha$ Syn and RFP proteins in W303.1A cells within a microchannel (width= 5 $\mu$ m) when subject to galactose induction. a) Visible micrograph of cells previously selected within microchannels at t=0h. b) Fluorescence micrograph of cells expressing RFP protein at t=0h. c) Fluorescence micrographs of cells expressing GFP- $\alpha$ Syn protein at t=0h d) 1.5h and e) 3h.

Looking at the previous figures one can immediately verify the heterogeneity of the results obtained in terms of protein expression levels in the strain W303.1A.

Starting with the analysis of the RFP protein, we can conclude that in the absence of methionine the cells express this protein as it was expected. However, RFP expression levels varied between individual cells. Gene expression is already known to vary stochastically between individual cells [29,30]. The reactions underlying gene expression involve small numbers of molecules (e.g., transcription factors, DNA, and mRNAs) and may therefore exhibit stochastic fluctuations that could generate population variation when phenotypic diversity would be advantageous.

The type of transformation based on plasmids, instead of the integration into the genome, could explain in part the variability of the expression levels between individual cells since the copy number per cell could vary over a population of cells and therefore the expression levels of the proteins could also be different. To eliminate this variability, some experiments with cells carrying two copies of  $\alpha$ syn-GFP inserted directly in the genome (strain VSY72) were performed to compare the variability of expression levels among individual cells inside microchannels.

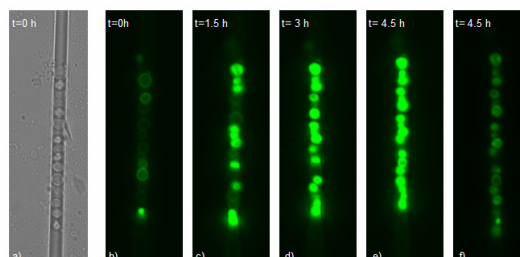


**Figure 11** - Expression levels of  $\alpha$ Syn-GFP protein in VSY72 cells within a microchannel (width= 5 $\mu$ m) when subject to galactose induction. a) Visible micrograph of cells previously selected within a microchannel at t=0h. b) Fluorescence micrographs of cells at t=0h, c) t= 1.5h d) t= 3h and e) t= 4.5h with an exposure time of 194ms. f) Fluorescence micrographs of cells at t=4.5h with an exposure time of 87ms.

We can clearly see that at *time zero* some cells have already started to express  $\alpha$ Syn-GFP in the plasma membrane but in reduced levels. The expression increased gradually and after 4.5 hours all the cells expressed this protein almost at the same intensity. The expression levels are so high that it was difficult to localize the origin of such fluorescence inside the cells using the same exposure time as at t=0h. For this reason, at 4.5 hours another image was acquired but with a lower exposure time to confirm that the fluorescence was located the plasma membrane.

Comparing the previous results to those referred to the cells carrying GFP- $\alpha$ Syn in a 2 $\mu$  plasmid, we can immediately verify the enormous

difference in terms of protein expression variability. All the cells that have two copies of such protein in the genome presented a very similar level of fluorescence intensity that did not happen in the cells carrying 2 $\mu$  plasmids. Therefore, we can conclude that for future studies involving the comparison of the expression levels of such protein when subject to a certain molecular gradient, the insertion of the genome is a better choice since the variability factor associated with the plasmid maintenance and copy number per cell is eliminated.

### 3.3. Generation of a stable gradient within microchannels

The microfluidic device developed in the present work was capable of generating gradients across microchannels between inlet and outlet reservoirs. Convective flow into the microchannels was minimized by designing the height of the channels (6 $\mu$ m) to be significantly smaller than the reservoirs (700 $\mu$ m). This large difference yields an even greater difference in fluidic resistance, causing flow to take the path of least resistance rather than entering the channels, allowing only diffusive transport.

The generation of stable gradients inside microchannels was maintained by constantly withdrawing the fluids from the reservoirs using the syringe pump. Continuously replenished source and sink is advantageous over static reservoirs because their concentration can be kept constant, and thus the gradients can be maintained at a constant profile in steady-state (Figure 12).

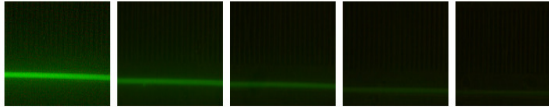


Figure 12 - FITC gradient inside a microchannel.

The optimal flow rate, in which the time window for the gradient was approximately the time necessary for the cells to express/repress the proteins according to the inducible/repressible gradient, was 5.5  $\mu$ L/min.

Initially, the flow rates were set to be constant in the inlet and outlet reservoirs. However, during the experiments using FITC it was verified that after the fluorophore crossed the channels it started to accumulate on the outlet reservoir close to the end of the channels (due to the small flow rate) and thus the diffusion phenomenon inverted direction and FITC molecules started to diffuse to the opposite side. To overcome this situation, one had to increase the flow rate of the solution (buffer) in the outlet reservoir in order to avoid FITC accumulation. The solution found to increase the flow rate in only one reservoir was to

use a syringe with a greater capacity (3mL) compared to the one used for the inlet reservoir (1mL). This way, the flow rate on the outlet reservoir was three times higher compared to the flow rate on the inlet reservoir, which allows the renewal of the solution faster than the one in the inlet reservoir.

It must be emphasized that the gradient stability is dependent on the flow, and remains stable as long as the flow is maintained in the reservoirs. The flow rates and outside reservoir volumes determine the time window for stable gradients. With outside reservoirs with volumes of 2 mL and flow rates of 5.5  $\mu$ L/min and 20  $\mu$ L/min in inlet and outlet reservoir respectively, the gradients can be maintained for 2,5 h.

By looking at the figure 13 it was possible to verify that a steady-state gradient was achieved, because the gradient remained stable, after 16 minutes.

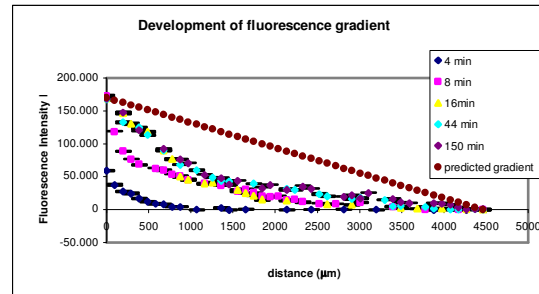


Figure 13 - Chart showing the fluorescence intensity profile across a microchannel (width=6  $\mu$ m) at different times. A stable gradient was established after 16 minutes.

However, the experimental results were not in good agreement with the theoretical predictions. After reaching a steady-gradient, a linear concentration of the fluorophore should have been established (see predicted gradient in Figure 12), according to the following equation [28]:

$$C = \frac{(C_r - C_l)}{L} x + C_l \quad (5)$$

where C is the concentration of the diffusing molecule, C<sub>r</sub> is the concentration in the inlet reservoir, C<sub>l</sub> is the concentration in the outlet reservoir, L is the length of the channel and x is the position across the channel.

We believe such deviations could be mainly attributed to the following aspects:

- Imperfections in the microchannels resulting from the lithography process.
- Convection was not completely eliminated inside microchannels. Despite the fact that the convection was minimized due to the design of the microfluidic device, it could also be possible that this phenomenon could not have been completely avoided and thus the gradient was not generated only by diffusion



transport across the microchannels.

- The fact that the syringe pump works with a stepper motor may also have led to deviations from the theoretical predictions because both FITC solution and buffer crossed the reservoirs not in continuous flow but in discrete steps.

#### 4. Conclusion

A new method to fabricate the master mold was implemented in which it is not necessary to make a photomask because the positive patterning is directly made by double exposure on a Direct Laser machine (DWL). Using this new method, the time spent to produce the microfluidic device decreased significantly. This new methodology allowed us to overcome many drawbacks of the traditional master mold techniques, including the obtaining of very small structures ( $\leq 10\mu\text{m}$ ).

The fabrication of microfluidic devices in PDMS had shown to present several advantages when compared to the devices made of glass or silicon, particularly in biological applications, a device should only be used once per experiment because it is very difficult to wash it and almost impossible to ensure that no cells were adhered to the glass or to the PDMS surface and therefore, using elastomeric materials like PDMS make all the process more cost effective.

The study of single *Saccharomyces cerevisiae* cells inside a microfluidic platform allowed us to understand some fundamental aspects in the field of Biology that would be impossible to comprehend in the traditional *macro* culture techniques. One of these essential aspects was the cellular heterogeneity among a population of cells carrying  $2\mu$  plasmids in terms of fluorescence protein expression levels. This variability decreased significantly in cells carrying the gene encoding the protein of interest directly in the genome. In accordance with the objectives of the present work, the cells that will be more useful will be the ones with genomic insertions of the SNCA gene.

Furthermore, with this device it was also possible to visualize other important aspects such the division time of a particular cell within microchannels and the successive generations of the same cell in a very controlled environment. The increasing in the division time of VSY72 cells comparing to WT cells proved the toxicity of  $\alpha\text{Syn}$  when overexpressed.

#### 5. Future Work Perspectives

In the short term some measurements and changes could be made in order to improve the results in the present project:

- Fabricate a microfluidic device with microchannels with a wide range of lengths and

widths. Possibly one could find the optimal length in which the steady-state gradient is linear.

- Find a way to immobilize the cells inside the microchannels either by hydrodynamic trapping, improving the methodology that we started by narrowing the channels in specific places or including more complex mechanical barriers/obstacles, or by chemical trapping.

In the long term, it would be advantageous to integrate in the device some other components besides microchannels that would be very important for more accurate results:

- A temperature sensor that could maintain an optimal temperature for biological applications.
- PDMS microvalves to control the fluid flow in microchannels that could also act as switches.
- Fabricate a fully integrated device in which the reservoirs are made in PDMS and thus eliminating *ependorf* tubes to the setup. A similar approach to the one showed in the following figure could be implemented.

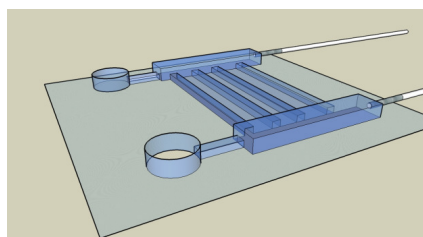


**Figure 14** - Long term microfluidic platform.

In biological terms, a long term line to follow would be:

- Creating an inducer gradient inside the channel that will stimulate *S. cerevisiae* to express  $\alpha\text{-syn}$  at different levels depending on the location of these cells along the microchannel.

The goal described above have in mind the future utilization of this microfluidic platform to test different proteins that are known to suppress  $\alpha\text{-syn}$  toxicity [31], by having the genes encoding these proteins under the control of repressible promoters. The subsequent creation of a new gradient of the respective repressor in the same channel will make it possible to analyse cell growth and generation time according to different levels respectively of  $\alpha\text{-syn}$  and suppressors (Figure 1.11). Accordingly, the final goal would be to find the optimal suppressor that would be able to recover cells sensing advance stages of  $\alpha\text{-syn}$  toxicity.

#### 6. References

- [1] G. M. Whitesides. The origins and the future of microfluidics. *NATURE*, 442(2006).

- [2] F. A. Gomez. Biological applications of Microfluidics. ed., John Wiley & Sons, Inc., 2008.
- [3] J. C. McDonald, D. C. Duffy, J. R. Anderson, D. T. Chiu, H. Wu, O. J. Schueller, G. M. Whitesides. Fabrication of microfluidic systems in poly(dimethylsiloxane). *Electrophoresis*, 2000, 21, 27-40.
- [4] J. Ouellette. A new wave of microfluidic devices. *American Institute of Physics*. 2003, 14-17.
- [5] B. Michel, A. Bernard, A. Bietsch, E. Delamarche, M. Geissler, D. Juncker, H. Kind, J.-P. Renault, H. Rothuizen, H. Schmid, P. Schmidt-Winkel, R. Stutz, H. Wolf. Printing meets lithography: Soft approaches to high-resolution patterning, *IBM J. RES. & DEV.*, 2001, Vol. 45, No. 5.
- [6] B. Michel. Printing Meets Lithography. *American Institute of Physics*, 2002
- [7] Y. Xia and G. M. Whitesides. Soft Lithography. *Annu. Rev. Mater. Sci.* 1998, 28,153–84.
- [8] D.Longo, J. Hasty. Dynamics of single-cell gene expression. *Molecular Systems Biology*. 2006, 64.
- [9] S. Cookson, N. Ostroff, W. L. Pang, D. Volfson, J. Hasty. Monitoring dynamics of single-cell gene expression over multiple cell cycles. *Molecular Systems Biology*. 2005.
- [10] J. Ryley, O. M. Pereira-Smith. Microfluidics device for single cell gene expression analysis in *Saccharomyces cerevisiae*. *Yeast*. 2006; 23: 1065–1073.
- [11] N. L. Jeon , H. Baskaran , SK. Dertinger , GM. Whitesides , L. Van de Water , M. Toner . Neutrophil chemotaxis in linear and complex gradients of interleukin-8 formed in a microfabricated device. *Nat. Biotechnol.*, 2002, 20(8), 826–830.
- [12] H. Mao, P. S. Cremer, M. D. Manson, A sensitive, versatile microfluidic assay for bacterial chemotaxis, *Proc. Natl. Acad. Sci. U. S. A.*, 2003, 100(9), 5449–5454.
- [13] J. Diao, L. Young, S. Kim, E. A. Fogarty, S. M. Heilman, P. Zhou, M. L. Shuler, M. W., M. P. DeLisa. A three-channel microfluidic device for generating static linear gradients and its application to the quantitative analysis of bacterial chemotaxis, *Lab Chip*, 2006, 6(3), 381–388.
- [14] S. Koyama, D. Amarie, H. A. Soini, M. V. Novotny, S. C. Jacobson. Chemotaxis assays of mouse sperm on microfluidic devices, *Anal. Chem.*, 2006, 78(10), 3354–3359.
- [15] W. Saadi, S. Wang, F. Lin, N. L. Jeon. A parallel-gradient microfluidic chamber for quantitative analysis of breast cancer cell chemotaxis, *Biomed. Microdev.*, 2006, 8(2), 109–118.
- [16] G. M. Walker, M. S. Ozers, D. J. Beebe. Cell infection within a microfluidic device using virus gradients. *Sens. Actuators B: Chem.*, 2004, 98(2–3), 347–355.
- [17]<http://www.yeastgenome.org/VLwhatareyeast.html>.
- [18] A. Gofieau, B. G. Barrell, H. Bussey, R. W. Davis, B. Dujon, H. Feldmann, F. Galibert, J. D. Hoheisel, C. Jacq, M. Johnston, E. J. Louis, H. W. Mewes, Y. Murakami, P. Philippsen, H. Tettelin, S. G. Oliver, *Life with 6000 genes*. *Science*, 1997, Volume 274, Issue 5287, 546,563-567.
- [19][http://www.sfn.org/index.cfm?pagename=brainBriefings\\_alphaSynucleinAndParkinsonsDisease](http://www.sfn.org/index.cfm?pagename=brainBriefings_alphaSynucleinAndParkinsonsDisease)
- [21] <http://nmnf.epfl.ch/page9109.html>
- [22] [www.dowcorning.com](http://www.dowcorning.com)
- [23] B. J. Thomas, R. Rothstein. *Genetics*. 1989,123, 725.
- [24] A. M. Taylor, Blurton-Jones, S. W. Rhee, D. H. Cribbs, C. W. Cotman, N. L. Jeon. A microfluidic platform for CNS axonal injury, regeneration and transport. *Nature Methods*. 2005, Vol. 2 n°8, 599-605.
- [25] N. L. Jeon , H. Baskaran , SK. Dertinger , GM. Whitesides , L. Van de Water , M. Toner . Neutrophil chemotaxis in linear and complex gradients of interleukin-8 formed in a microfabricated device. *Nat. Biotechnol.*, 2002, 20(8), 826–830.
- [26] B. Mosadegh, C. Huang, J. W. Park, H. S. Shin, B. G. Chung, S. Hwang, K. Lee, H. J. Kim, J. Brody, N. L. Jeon. Generation of Stable Complex Gradients Across Two-Dimensional Surfaces and Three-Dimensional Gels. *Langmuir*. 2007, 23, 10910-10912.
- [27] C. Yi, C. Li, S. Ji, M. Yang. Microfluidics technology for manipulation and analysis of biological cells. *Analytica Chimica Acta*, 560 (2006), 1–23.
- [28] G.M. Walker, M.S. Ozers, D.J. Beebe. Insect cell culture in microfluidic channels. *Biomed. Microdevices*. 2002, 4, 161.
- [29] J. M. Raser, E. K. O'Shea. Control of Stochasticity in Eukaryotic Gene Expression. *Science*. 2004 June 18; 304(5678): 1811–1814.
- [30] E. M. Ozbudak, M. Thattai, I. Kurtser, A. D. Grossman, A. van Oudenaarden. Regulation of noise in the expression of a single gene. *Nature Genetics*. May 2002,31, 69-73.
- [31] S. Willingham, T. F. Outeiro, M. J. DeVit, S. L. Lindquist, P. J. Muchowski. Yeast Genes That Enhance the Toxicity of a Mutant Huntingtin Fragment or  $\alpha$ -Synuclein. *Science*. 2003 December 5; 302(5651): 1769–1772.

